Two-dimensional localized vibrational modes of *trans*-$(CH)_x$ around a soliton

Z. J. Li and Biao Xing
Department of Physics, Huazhong University of Science and Technology, Wuhan, People's Republic of China

K. L. Yao
Center of Theoretical Physics, Chinese Center of Advanced Science and Technology (World Laboratory), Beijing, People's Republic of China and Department of Physics, Huazhong University of Science and Technology, Wuhan, People's Republic of China

(Received 19 November 1990)

We assess the influence of the polyacetylene configuration on the localized vibrational modes of a soliton. The bond-bending effect is also included within the framework of a previously published two-dimensional model [Phys. Rev. B **42**, 2084 (1990)]. A number of these additional modes have been found, compared with results based on the Su-Schrieffer-Heeger model. They depend on both the coupling constant and bond-bending term.

A fascinating phenomenon which has been observed in experiments on a number of conjugated polymers is that nonlinear excitations, either by doping[1,2] or photoexcitation,[3,4] induce additional features in the infrared-absorption spectra. These features are believed to result from localized vibrations of polymer around the defects.[5] Theoretical analyses of this phenomenon have mainly focused on polyacetylene as a simple prototypical system. A series of elegant calculations have been performed, based on the Su-Schrieffer-Heeger (SSH) model[6] and its continuum version Takayama-Lin-liu-Maki (TLM) model.[7] Four localized vibrational modes for a soliton of the coupling constant $\lambda=0.19$ have been found.[5,8–16] Three of them are ir active, two of which have large oscillator strength. These modes do not have direct experimental correspondings since the in-plane lattice degrees of freedom are neglected. The coupling of three lattice degrees of freedom to the zero-frequency uniform translational mode [Alexander-McTague (AM) formalism] due to Horovitz[8] and the nonuniform translational mode due to Mele and Hicks[9] and Terai *et al.*[14] have been proposed to explain the experimental results.

Thus, it is natural to go beyond one-dimensional theories as two of us have done in the polaron case.[17] The result shows that when the in-plane degrees of freedom are included, vibrations normal to the $(CH)_x$ chain and along the chain become comparable. In this work, we will continue our investigations for the soliton case, based on a previous paper.[17]

The Hamiltonian reads

$$H=-\sum_{n,s}(t_0-\alpha\delta r_{n,n+1})(c^{\dagger}_{n+1,s}c_{n,s}+\text{H.c.}) +\frac{k}{2}\sum_n(\delta r_{n,n+1})^2+\frac{k'}{2}\sum_n(\delta\theta_n)^2+\frac{M}{2}\sum_n(\dot{r}_n)^2 , \tag{1}$$

where t_0, α, k, M have the same conventional meanings as in the SSH model. k' is the spring constant of the bond-bending term. $\delta r_{n,n+1}$ denotes the change of bond length from the equilibrium position between the nth and $(n+1)$-th site. We introduce the following dimensionless parameters:

$$\delta U_{n,n+1}=\frac{\alpha}{t_0}\delta r_{n,n+1} , \quad \lambda=\frac{2\alpha^2}{\pi k t_0} , \quad \tau=\omega_Q t , \quad \tilde{k}=k/t_0 , \tag{2}$$

where $\omega_Q=(4k/M)^{1/2}$ is the bare frequency. Equation (1) can be rewritten as

$$H/t_0=-\sum_{n,s}(1-\delta U_{n,n+1})(c^{\dagger}_{n+1,s}c_{n,s}+\text{H.c.}) +\frac{1}{\pi\lambda}\sum_n(\delta U_{n,n+1})^2+\frac{1}{\pi\lambda}\sum_n(\dot{U}_n)^2 +\frac{\tilde{k}}{2}\sum_n(\delta\theta_n)^2 , \tag{3}$$

where $\dot{U}_n=dU_n/d\tau$. This shows that, if the energy is measured in units of t_0 and frequency in units of ω_Q, then the properties of system will only depend on the coupling constant λ and $\tilde{k}$.

A static solution of the soliton, which is irrelevant to the bond-bending term and similar to previous results,[6,18] can be determined by the following self-consistent equations:

$$\varepsilon_i\phi_i(n)=-(1-\delta U_{n,n-1})\phi_i(n-1)(1-\delta_{n,1}) -(1-\delta U_{n,n+1})\phi_i(n+1)(1-\delta_{n,N}) , \quad \delta U_{n,n+1}=-\pi\lambda\left[\sum_n\phi_i(n)\phi_i(n+1)-2/\pi\right] , \tag{4}$$

where the open chain boundary condition has been

TABLE I. Localized vibrational modes around a soliton for $\lambda=0.19$ and $\tilde{k}=0$. $X^i_{\max}$ and $Y^i_{\max}$ denote the maximum amplitude of the ith mode in the x and y directions, respectively. The symmetry of the x (or y) amplitude for a given mode is specified relative to the center of the chain.

Localized mode	Frequency Ω_i/ω_Q	$X^i_{\max}$ (symmetry)	$Y^i_{\max}$ (symmetry)
G_1	0.000	0.306 (even)	0.023 (odd)
G_2	0.436	0.217 (odd)	0.094 (even)
G_3	0.477	0.105 (even)	0.152 (odd)
G_4	0.672	0.385 (even)	0.218 (odd)
G_5	0.692	0.284 (odd)	0.123 (even)
G_6	0.643	0.200 (odd)	0.140 (even)

used,[19] ε_i is the eigenvalue of the electron and $\phi_i(n)$ denotes the nth component of the electron eigenfunction. To reproduce the results of the SSH model, we choose

$$t_0=2.5 \text{ eV}, \quad \alpha=4.73 \text{ eV Å}^{-1}, \quad k=28 \text{ eV Å}^{-2},$$

which correspond to an energy gap $2\Delta=1.35$ eV, dimerization $\delta r=0.07$ Å, and coupling constant $\lambda=0.19$. We perform the calculation with 81 atoms, using the exact solution of the soliton in the TLM model to iterate. Finally, one will obtain the set of $\{\delta U^9_{n,n+1}\}$, which determines the soliton configuration located in the center of the chain.

To consider lattice vibration around a soliton, we follow the procedures described in a previous paper[17] and finally obtain the vibrational energy of the system:

$$E=E^s+\tfrac{1}{2}\sum_{m,n} V^{\alpha\beta}_{mn}\eta^\alpha_m\eta^\beta_n+\frac{4}{\pi\lambda}\sum_n(\dot{U}_n)^2 \tag{5}$$

in which $\alpha,\beta=1,2$ denote the x direction (along the chain) and y direction (normal to chain) respectively, and E^s is the energy of a soliton. One obtains all the vibrational modes by diagonalizing the matrix V_{mn}. The vibrational amplitude G_i corresponding to the frequency Ω_i can be expressed as

$$G_i\equiv[X(i),Y(i)]$$
$$=(X^i_1\cdots X^i_m\cdots X^i_{81},Y^i_1\cdots Y^i_m\cdots Y^i_{81}), \tag{6}$$

where X^i_m and Y^i_m stand for the vibrational amplitudes of the mth site in the x and y directions, respectively. Readers are referred to the Appendix for an explicit expression of $V^{\alpha\beta}_{mn}$.

Our calculation shows that, among 162 vibrational modes, 83 modes have zero frequency for $\tilde{k}=0$, one of which corresponds to Goldstone mode. Six localized modes have been found (see Table I), compared to four modes of the SSH model.[8–16] G_1 (Goldstone mode), G_2, G_3, and G_4 (staggered mode) have their correspondings in the one-dimensional results[8–16] according to the shapes of the x amplitudes. G_1, G_3, and G_4 are ir active, related to infrared absorption.[12] G_5 and G_6 are the additional ones found, whose shapes of amplitudes are shown in Figs. 1 and 2. No other additional localized modes occur for $\tilde{k}\le 0.6$, but the increasing of $\tilde{k}$ causes small shifts of frequencies of both extended and localized modes.

Nine localized modes have been found for $\tilde{k}=0.75$ (see Table II), and six of them (G_1–G_6) are just the modes found for $\tilde{k}=0$. The modes G_7–G_9 are the new localized modes. The shape of G_7 is shown in Fig. 3. When $\tilde{k}=1.0$, 12 localized modes have been found (see Table III), and, again, six of them have existed in the case of $\tilde{k}=0$. G''_7–G''_{12} are the additional localized modes (G''_7 is shown in Fig. 4).

It is worth noting that the modes G_1–G_6 always exist in our calculation and frequencies of G_1, G_4, G_5, and G_6 do not change, to our precision, for different $\tilde{k}$. The X and Y amplitudes of any modes have inverse symmetry about the center of the chain, and the amplitudes of both

TABLE II. Localized vibrational modes around a soliton for $\lambda=0.19$ and $\tilde{k}=0.75$. $X^i_{\max}$ and $Y^i_{\max}$ denote maximum amplitude of the ith mode in the x and y directions, respectively. The symmetry of the x (or y) amplitude for a given mode is specified relative to the center of the chain.

Localized mode	Frequency Ω_i/ω_Q	$X^i_{\max}$ (symmetry)	$Y^i_{\max}$ (symmetry)
G_1	0.000	0.332 (even)	0.097 (odd)
G_2	0.447	0.236 (odd)	0.034 (even)
G_3	0.516	0.190 (even)	0.048 (odd)
G_4	0.672	0.382 (even)	0.221 (odd)
G_5	0.692	0.261 (odd)	0.117 (even)
G_6	0.643	0.212 (odd)	0.158 (even)
G_7	0.621	0.080 (even)	0.236 (odd)
G_8	0.624	0.066 (odd)	0.199 (even)
G_9	0.620	0.056 (odd)	0.275 (even)

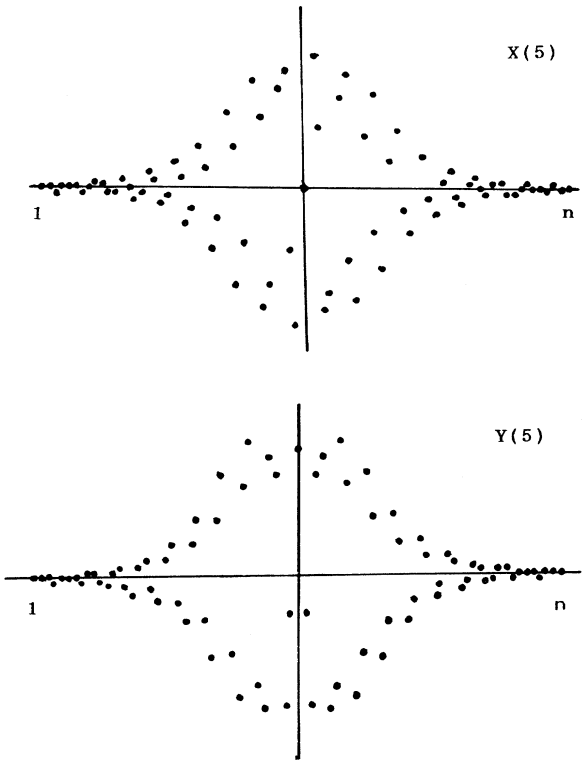

FIG. 1. Shape of the localized mode G_5 for $\tilde{k}=0$. The unit of the abscissa is site number n, and the ordinate is in an arbitrary unit.

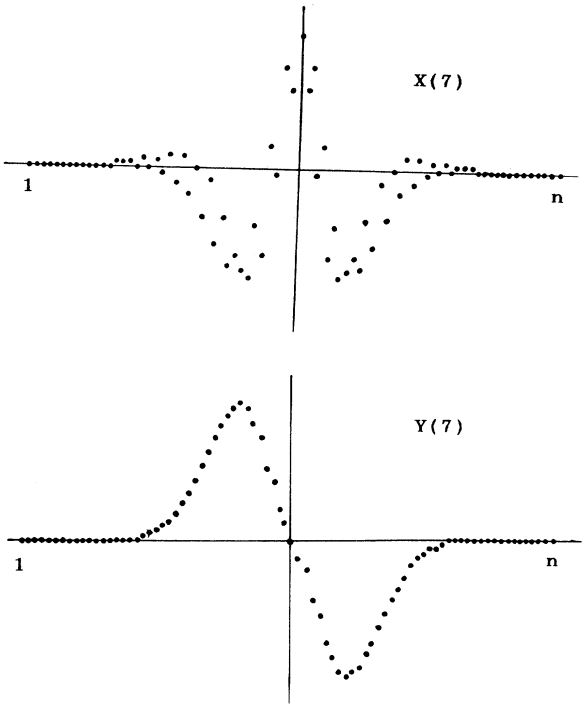

FIG. 3. The shape of the localized mode G_7 for $\tilde{k}=0.75$. The units of both axes are the same as in Fig. 1.

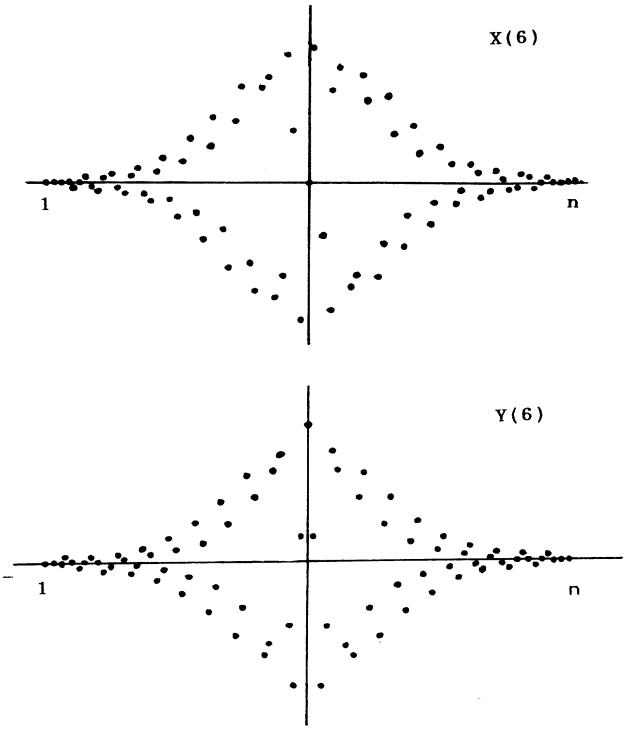

FIG. 2. The shape of the localized mode G_6 for $\tilde{k}=0$. The units of both axes are the same as in Fig. 1.

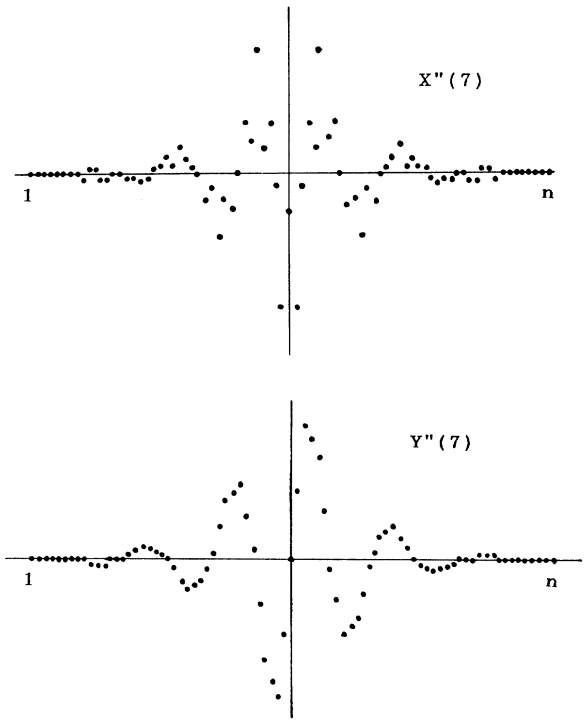

FIG. 4. The shape of the localized mode G_7'' for $\tilde{k}=1.0$. The units of both axes are the same as in Fig. 1.

TABLE III. Localized vibrational modes around a soliton for $\lambda=0.19$ and $\tilde{k}=1.0$. $X^i_{\max}$ and $Y^i_{\max}$ denote the maximum amplitude of the ith mode in the x and y directions, respectively. The symmetry of the x (or y) amplitude for a given mode is specified relative to the center of the chain.

Localized mode	Frequency Ω_i/ω_Q	$X^i_{\max}$ (symmetry)	$Y^i_{\max}$ (symmetry)
G_1	0.000	0.300 (even)	0.116 (odd)
G_2	0.449	0.237 (odd)	0.028 (even)
G_3	0.518	0.192 (even)	0.035 (odd)
G_4	0.672	0.391 (even)	0.224 (odd)
G_5	0.692	0.250 (odd)	0.118 (even)
G_6	0.643	0.219 (odd)	0.168 (even)
G''_7	0.632	0.194 (even)	0.324 (odd)
G''_8	0.632	0.218 (odd)	0.346 (even)
G''_9	0.653	0.099 (odd)	0.307 (even)
G''_{10}	0.653	0.114 (even)	0.270 (odd)
G''_{11}	0.655	0.066 (odd)	0.225 (even)
G''_{12}	0.656	0.073 (even)	0.238 (odd)

directions for most of modes are comparable as in the polaron case.[17] Thus, we can conclude that the number of localized modes and their frequencies depend not only on the coupling constant,[8–16] but also on the bond-bending term. The exact value of k' for *trans*-$(CH)_x$ is unclear. If $\tilde{k}>0.6$ for polyacetylene, alternative ir active modes may contribute to the additional large absorptions observed in the experiment.[12] Electron-electron interactions are neglected in our calculation. Several authors have shown that electron-electron interactions and the pinning effect do not change the number of localized modes, although they cause shifts in frequencies.[20–22]

Finally, we would like to make some comparisons of our results with the original parametrized version of the continuum model by Horovitz[8] and related calculations.[9,14] According to these calculations,[8,9,14] the coupling of the lattice degrees of freedom, n, to one-dimensional localized vibrational modes will increase the number of localized modes n-fold ($n=3$ in these calculations) once the one-dimensional static solutions are fixed. But that is not the case in our calculation. The bond-bending term, which is irrelevant to static solutions, affects the localized modes in a way that does not increase the number of one-dimensional localized modes by a factor n, even when we have the same static solutions as that in the TLM or SSH models. Thus, our results argue that the localized modes by coupling lattice degrees of freedom to one-dimensional modes[8,9,14] may not be all localized.

This project was supported by the National Natural Science Foundation of China.

APPENDIX

In the following expression, $r_{n,n+1}$ denotes the bond length between the nth and $(n+1)$-th site and experimentally equals 1.4 Å in the case of undimerization. α and $\beta=1,2$ stand for the x and y directions, respectively, i.e., $\eta^1_m=X_m$ and $\eta^2_m=Y_m$. θ is half of a bond angle and equals 60°.

The vibrational matrix, including electron contribution (the first term), bond-stretching energy (the second term), and bond-bending energy (the last term), is expressed as

$$V^{\alpha\beta}_{mn}=2\sum_{\substack{i,s\\(\text{occ})}}\sum_{j\neq i}\frac{D^{m\alpha}_{ij}D^{n\beta}_{ij}}{\varepsilon_i-\varepsilon_j}+M^{\alpha\beta}_{mn}+M'^{\alpha\beta}_{mn}\ ,$$

$$D^{n\alpha}_{ij}=C^n_{ij}q^\alpha_n(1-\delta_{n1})-C^{n+1}_{ij}q^\alpha_{n+1}(1-\delta_{nN})\ ,$$

$$C^n_{ij}=\phi_i(n)\phi_j(n-1)+\phi_i(n-1)\phi_j(n)\ ,$$

$$q^1_n=\sin\theta,\quad q^2_n=(-1)^n\cos\theta\ ,$$

$$\begin{aligned}M^{\alpha\beta}_{mn}=\frac{2}{\lambda\pi}[\,&(2-\delta_{n1}-\delta_{nN})(\sin^2\theta\delta_{mn}\delta\alpha_1\delta\beta_1+\cos^2\theta\delta_{mn}\delta\alpha_2\delta\beta_2)\\&+(\delta_{nN}-\delta_{n1})\sin\theta\cos\theta(-1)^n\delta_{mn}\delta\alpha_1\delta\beta_2+(\delta_{nN}-\delta_{n1})\sin\theta\cos\theta(-1)^n\delta_{mn}\delta\alpha_2\delta\beta_1\\&-(1-\delta_{nN})\sin^2\theta\delta_{m,n+1}\delta\alpha_1\delta\beta_1-(1-\delta_{n1})\sin^2\theta\delta_{m,n-1}\delta\alpha_1\delta\beta_1\\&-(1-\delta_{nN})\cos^2\theta\delta_{m,n+1}\delta\alpha_2\delta\beta_2-(1-\delta_{n1})\cos^2\theta\delta_{m,n-1}\delta\alpha_2\delta\beta_2\\&-(1-\delta_{nN})\sin\theta\cos\theta(-1)^{n+1}\delta_{n+1,m}\delta\alpha_1\delta\beta_2-(1-\delta_{n1})\sin\theta\cos\theta(-1)^n\delta_{n-1,m}\delta\alpha_2\delta\beta_1\\&-(1-\delta_{n,N})\sin\theta\cos\theta(-1)^{n+1}\delta_{n+1,m}\delta\alpha_1\delta\beta_1-(1-\delta_{n1})\sin\theta\cos\theta(-1)^n\delta_{n-1,m}\delta\alpha_1\delta\beta_2]\ ,\end{aligned}$$

$$
\begin{aligned}
M'^{\alpha\beta}_{m,n} = {} & \frac{\tilde{k}}{3}\sin^2\theta \left\{ \frac{1}{r^2_{n,n-1}}(2-2\delta_{n1}-\delta_{nN}-\delta_{n2}) + \frac{1}{r^2_{n+1,n}}(2-2\delta_{nN}-\delta_{n,N-1}-\delta_{n1}) \right. \\
& \left. - \frac{2}{r_{n,n-1}r_{n+1,n}}(1-\delta_{n1}-\delta_{nN}) \right\} \delta_{mn}\delta\alpha_1\delta\beta_1 \\
& - \frac{\tilde{k}}{3}\sin^2\theta \left\{ \frac{1}{r^2_{n+1,n}}(2-2\delta_{nN}-\delta_{n,N-1}-\delta_{n1}) - \frac{1}{r_{n,n-1}r_{n+1,n}}(1-\delta_{n1}-\delta_{nN}) \right. \\
& \left. - \frac{1}{r_{n+1,n}r_{n+2,n+1}}(1-\delta_{nN}-\delta_{nN-1}) \right\} \delta_{m,n+1}\delta\alpha_1\delta\beta_1 \\
& - \frac{\tilde{k}}{3}\sin^2\theta \left\{ \frac{1}{r^2_{n+1,n}}(2-2\delta_{n1}-\delta_{nN}-\delta_{n2}) - \frac{1}{r_{n-1,n-2}r_{n,n-1}}(1-\delta_{n1}-\delta_{n2}) \right. \\
& \left. - \frac{1}{r_{nn-1}r_{n+1,n}}(1-\delta_{n1}-\delta_{nN}) \right\} \delta_{m,n-1}\delta\alpha_1\delta\beta_1 \\
& - \frac{\tilde{k}}{3}\sin^2\theta \left\{ \frac{\delta_{m,n+2}}{r_{n+1,n}r_{n+2,n+1}}(1-\delta_{nN}-\delta_{nN-1}) + \frac{\delta_{m,n-2}}{r_{n-1,n-2}r_{n,n-1}}(1-\delta_{n1}-\delta_{n2}) \right\} \delta\alpha_1\delta\beta_1 \\
& + 3\tilde{k}\cos^2\theta \left\{ \frac{1}{r^2_{n,n-1}}(2-2\delta_{n1}-\delta_{n2}-\delta_{nN}) + \frac{1}{r^2_{n+1,n}}(2-2\delta_{nN}-\delta_{n1}-\delta_{n,N-1}) \right. \\
& \left. + \frac{2}{r_{n,n-1}r_{n+1,n}}(1-\delta_{n1}-\delta_{nN}) \right\} \delta_{m,n}\delta\alpha_2\delta\beta_2 \\
& - 3\tilde{k}\cos^2\theta \left\{ \frac{1}{r^2_{n+1,n}}(2-2\delta_{nN}-\delta_{n,N-1}-\delta_{n1}) + \frac{1}{r_{n,n-1}r_{n+1,n}}(1-\delta_{n1}-\delta_{nN}) \right. \\
& \left. + \frac{1}{r_{n+1,n}r_{n+2,n+1}}(1-\delta_{nN}-\delta_{n,N-1}) \right\} \delta_{m,n+1}\delta\alpha_2\delta\beta_2 \\
& - 3\tilde{k}\cos^2\theta \left\{ \frac{1}{r^2_{n,n-1}}(2-2\delta_{n1}-\delta_{n2}-\delta_{nN}) + \frac{1}{r_{n,n-1}r_{n-1,n-2}}(1-\delta_{n1}-\delta_{n2}) \right. \\
& \left. + \frac{1}{r_{n,n-1}r_{n+1,n}}(1-\delta_{n1}-\delta_{nN}) \right\} \delta_{m,n-1}\delta\alpha_2\delta\beta_2 \\
& + 3\tilde{k}\cos^2\theta \left\{ \frac{\delta_{m,n+2}}{r_{n+1,n}r_{n+2,n+1}}(1-\delta_{nN}-\delta_{n,N-1}) + \frac{\delta_{m,n-2}}{r_{n,n-1}r_{n-1,n-2}}(1-\delta_{n1}-\delta_{n2}) \right\} \delta\alpha_2\delta\beta_2 \\
& + \tilde{k}\sin\theta\cos\theta \left\{ \frac{(-1)^{n-1}}{r^2_{n,n-1}}(2-2\delta_{n1}-\delta_{n2}-\delta_{nN}) + \frac{(-1)^n}{r^2_{n+1,n}}(2-2\delta_{n,N}-\delta_{n1}-\delta_{n,N-1}) \right\} \delta_{mn}\delta\alpha_1\delta\beta_2 \\
& + \tilde{k}\sin\theta\cos\theta \left\{ \frac{(-1)^{n-1}}{r^2_{n,n-1}}(2-2\delta_{n1}-\delta_{n2}-\delta_{nN}) + \frac{(-1)^n}{r^2_{n+1,n}}(2-2\delta_{nN}-\delta_{n1}-\delta_{n,N-1}) \right\} \delta_{mn}\delta\alpha_2\delta\beta_1 \\
& - \tilde{k}\sin\theta\cos\theta \left\{ \frac{(-1)^n}{r^2_{n+1,n}}(2-2\delta_{nN}-\delta_{n1}-\delta_{n,N-1}) - \frac{(-1)^{n+1}}{r_{n,n-1}r_{n+1,n}}(1-\delta_{n1}-\delta_{n,N}) \right. \\
& \left. - \frac{(-1)^n}{r_{n+1,n}r_{n+2,n+1}}(1-\delta_{nN}-\delta_{nN-1}) \right\} \delta_{m,n+1}\delta\alpha_1\delta\beta_2 \\
& - \tilde{k}\sin\theta\cos\theta \left\{ \frac{(-1)^{n-1}}{r^2_{n,n-1}}(2-2\delta_{n1}-\delta_{n,N}-\delta_{n2}) - \frac{(-1)^{n-1}}{r_{n,n-1}r_{n-1,n-2}}(1-\delta_{n1}-\delta_{n2}) \right. \\
& \left. - \frac{(-1)^n}{r_{n,n-1}r_{n+1,n}}(1-\delta_{n1}-\delta_{nN}) \right\} \delta_{m,n-1}\delta\alpha_1\delta\beta_2
\end{aligned}
$$

$$-\tilde{k}\sin\theta\cos\theta\left[\frac{(-1)^n}{r_{n+1,n}^2}(2-2\delta_{n,N}-\delta_{n,N-1}-\delta_{n1})-\frac{(-1)^n}{r_{n,n-1}r_{n+1,n}}(1-\delta_{n1}-\delta_{nN})\right.$$
$$\left.-\frac{(-1)^{n+1}}{r_{n+1,n}r_{n+2,n+1}}(1-\delta_{nN}-\delta_{n,N-1})\right]\delta_{m,n+1}\delta\alpha_2\delta\beta_1$$
$$-\tilde{k}\sin\theta\cos\theta\left[\frac{(-1)^{n-1}}{r_{n,n-1}^2}(2-2\delta_{n1}-\delta_{nN}-\delta_{n2})-\frac{(-1)^n}{r_{n,n-1}r_{n-1,n-2}}(1-\delta_{n1}-\delta_{n2})\right.$$
$$\left.-\frac{(-1)^{n+1}}{r_{n,n-1}r_{n+1,n}}(1-\delta_{n1}-\delta_{nN})\right]\delta_{m,n-1}\delta\alpha_2\delta\beta_1$$
$$-\tilde{k}\sin\theta\cos\theta\left[\frac{(-1)^n}{r_{n+1,n}r_{n+2,n+1}}\delta_{m,n+2}(1-\delta_{nN}-\delta_{n,N-1})+\frac{(-1)^{n-1}}{r_{n,n-1}r_{n-1,n-2}}\delta_{m,n-2}(1-\delta_{n1}-\delta_{n2})\right]\delta\alpha_1\delta\beta_2$$
$$-\tilde{k}\sin\theta\cos\theta\left[\frac{(-1)^n}{r_{n,n-1}r_{n-1,n-2}}\delta_{m,n-2}(1-\delta_{n1}-\delta_{n2})+\frac{(-1)^{n+1}}{r_{n+1,n}r_{n+2,n+1}}\delta_{m,n+2}(1-\delta_{nN}-\delta_{n,N-1})\right]\delta\alpha_2\delta\beta_1 .$$

[1]C. R. Fincher, Jr., M. Ozaki, A. J. Heeger, and A. G. MacDiarmid, Phys. Rev. B **19**, 4140 (1979).

[2]S. Etemad, A. Pron, A. J. Heeger, A. G. MacDiarmid, E. J. Mele, and M. J. Mele, Phys. Rev. B **23**, 5137 (1981).

[3]Z. Vardeny, J. Orenstein, and G. L. Baker, Phys. Rev. Lett. **50**, 2032 (1983).

[4]G. B. Blanchet, C. R. Fincher, T. C. Chung, and A. J. Heeger, Phys. Rev. Lett. **50**, 1938 (1983).

[5]E. J. Mele and M. J. Rice, Phys. Rev. Lett. **45**, 926 (1980).

[6]W. P. Su, J. R. Schrieffer, and A. J. Heeger, Phys. Rev. B **22**, 2099 (1980).

[7]H. Takayama, Y. R. Lin-liu, and K. Maki, Phys. Rev. B **21**, 2388 (1980).

[8]B. Horovitz, Solid State Commun. **41**, 29 (1982).

[9]E. J. Mele and J. C. Hicks, Phys. Rev. B **32**, 2704 (1985); J. C. Hicks and E. J. Mele, *ibid.* **34**, 1091 (1986).

[10]H. Ito, A. Terai, Y. Ono, and Y. Wada, J. Phys. Soc. Jpn. **53**, 3520 (1984); A. Terai, H. Ito, Y. Ono, and W. Wada, *ibid.* **54**, 196 (1985).

[11]J. Hicks and G. Blaisdell, Phys. Rev. B **31**, 919 (1985).

[12]H. E. Schaffer, R. H. Friend, and A. J. Heeger, Phys. Rev. B **36**, 7537 (1987).

[13]X. Sun, C. Q. Wu, and X. Shen, Solid State Commun. **56**, 1039 (1985).

[14]A. Terai, Y. Ono, and Y. Wada, J. Phys. Soc. Jpn. **55**, 2889 (1986); A. Terai and Y. Ono, *ibid.* **55**, 213 (1986).

[15]K. A. Chao and Y. J. Wang, J. Phys. C **18**, L1127 (1985).

[16]J. Tinka Gammel and J. C. Hicks, Synth. Met. **17**, 63 (1987).

[17]Biao Xing and K. L. Yao, Phys. Rev. B **42**, 2084 (1990).

[18]S. Stafstrom and K. A. Chao, Phys. Rev. B **29**, 7010 (1984); **30**, 2098 (1984).

[19]W. P. Su, Solid State Commun. **35**, 899 (1980).

[20]C. Q. Wu and X. Sun, Phys. Rev. B **33**, 8772 (1986).

[21]Richard J. Cohen and Arnold J. Glick, Phys. Rev. B **36**, 2907 (1987).

[22]J. C. Hicks and J. T. Gammel, Phys. Rev. B **37**, 6315 (1988).